RESOURCE ALLOCATION FOR OFDM-BASED DOWNSTREAM MULTI-USER SIMULTANEOUS WIRELESS INFORMATION AND POWER TRANSFER

Richard Ketcham, Jeroen Verdyck, and Marc Moonen

KU Leuven, Department of Electrical Engineering (ESAT),
STADIUS Center for Dynamical Systems, Signal Processing and Data Analytics

ABSTRACT

This paper considers a resource allocation method to simultaneously optimize the beamforming vectors and power allocation for downstream multi-user simultaneous wireless information and power transfer (SWIPT) systems that employ orthogonal frequency division multiplexing (OFDM). The method utilizes a novel MAC-BC duality to simplify an optimization problem composed of a weighted-sum of data rates subject to power harvesting and transmit power constraints. A simple method to dynamically choose the minimum harvesting power instead of using a constant value is also introduced. In simulations, it is observed that the resulting rate-power region appears to be convex.

***Index Terms*—** SWIPT, OFDM, Resource Allocation, Optimization, Precoding

1. INTRODUCTION

This paper presents a method to simultaneously optimize the beamforming vectors and power allocation for downstream multi-user SWIPT systems that employ OFDM. The concurrent nature of SWIPT makes optimal resource allocation challenging and an area of ongoing research, some of which examines using OFDM ([1], [2], [3]). Most similar to our work, [2] considers a network using beamforming vectors, but does not optimize them and instead assumes the beamforming vectors are given. This assumption may lead to a suboptimal solution since the design of the beamforming vectors changes significantly depending on if the system seeks to promote information transfer, power transfer, or a combination of the two. There has been work in which the beamforming vector optimization and power allocation is jointly considered for the single carrier case ([4], [5], [6]), but to the authors' knowledge beamforming optimization has not been considered for multi-user SWIPT networks using OFDM.

OFDM enables the use of a Lagrange dual-based algorithm since multicarrier systems have zero duality gap, which then enables the use of a MAC-BC duality. First an optimization problem is formulated in which a weighted-sum of the data rates is maximized subject to power harvesting and transmit power constraints. A novel simplification via a MAC-BC duality is then utilized to solve the Lagrange dual of the resource allocation problem. Lastly, a simple method to dynamically choose the minimum harvesting power is utilized in the simulations.

This research work was carried out at the ESAT Laboratory of KU Leuven, in the frame of:

Fonds de la Recherche Scientifique - FNRS and the Fonds Wetenschappelijk Onderzoek - Vlaanderen under EOS Project no 30452698 '(MUSE-WINET) MUlti-SErvice WIreless NETwork'

Research Project FWO nr. G.0B1818N 'Real-time adaptive cross-layer dynamic spectrum management for fifth generation broadband copper access networks'

The scientific responsibility is assumed by its authors.

2. SYSTEM MODEL

A SWIPT system using OFDM is considered, where the OFDM symbols are comprised of K orthogonal sub-carriers. The envisioned system is modeled by a network containing one access point using N_{T} antennas to deliver data and power to N remote devices each with one antenna, where $N \leq N_{\mathrm{T}}$. Additionally, it is assumed that there is no inter-carrier interference present, which allows each sub-carrier to be modeled independently and that perfect channel state information is available.

2.1. Downstream Channel

The access point applies a precoder to the symbol vector before transmitting to individual remote devices. This is commonly referred to as the broadcast channel (BC) and may be modeled on each sub-carrier (denoted with subscript k) as

$$y_k = H_k^{\mathcal{H}} T_k x_k + z_k. \tag{1}$$

Where $\mathbf{H_k^{\mathcal{H}}}$ is the the $N \times N_{\mathrm{T}}$ channel matrix, with $[\mathbf{H_k}]^{\mathcal{H}}_{\mathbf{m,n}}$ being the transfer function between receiver n and transmitter m, evaluated at sub-carrier k. Moreover, $\boldsymbol{z_k}$ is the $N \times 1$ additive white Gaussian noise, $\boldsymbol{x_k}$ is the $N \times 1$ vector of transmit symbols, $\mathbf{T_k}$ is the $N_{\mathrm{T}} \times N$ precoder matrix, and $\boldsymbol{y_k}$ is the $N \times 1$ vector of symbols as received by the remote devices.

2.2. Performance Metrics

For information transfer, the downstream data rate (DR) for user n on sub-carrier k may be modeled using Shannon's channel capacity equation divided by the sub-carrier bandwidth:

$$\alpha_n \log_2 \left(1 + \gamma_{k,n}^{\mathrm{DS}}(T_k, s_k)\right). \tag{2}$$

The downstream SINR for user n on sub-carrier k, $\gamma_{k,n}^{\mathrm{DS}}(\mathbf{T_k}, \boldsymbol{s_k})$, is a function of the precoder matrix, $\mathbf{T_k}$, and symbol power (SP) vector, $\boldsymbol{s_k}$. The SP for user n (i.e. the n-th element of $\boldsymbol{s_k}$) is denoted by $s_{k,n}$, where $s_{k,n} \triangleq \mathbb{E}\left[|x_{k,n}|^2\right]$ with $\mathbb{E}[\cdot]$ being the expected value operator. The term α_n is $\in [0, 1]$ and is included in the formulation to reflect reduced efficiencies due to the receiver architecture type (e.g. time-splitting), but will be omitted (i.e. effectively assumed

$\alpha_n = \alpha \ \forall \ n$) in Section (3) due to space. The downstream SINR is given by:

$$\gamma_{k,n}^{\mathrm{DS}}(T_k, s_k) = \frac{|t_{k,n}^{\mathcal{H}} h_{k,n}|^2 s_{k,n}}{\sum_{\substack{m=1 \\ m \neq n}}^{N} |t_{k,m}^{\mathcal{H}} h_{k,n}|^2 s_{k,m} + \sigma_{k,n}}, \tag{3}$$

where $\boldsymbol{t_{k,n}}$ is the precoder vector for user n (i.e. the n-th column of $\mathbf{T_k}$). The transfer function for user n (i.e. the n-th column of $\mathbf{H_k}$) is $\boldsymbol{h_{k,n}}$. The additive white Gaussian noise power spectral density experienced by user n and sub-carrier k is given by $\sigma_{k,n}$.

The power harvested by user m on sub-carrier k is

$$P_{k,m}(T_k, s_k) = (1 - \alpha_m) \sum_{n=1}^{N} |t_{k,n}^{\mathcal{H}} h_{k,m}|^2 s_{k,n}, \tag{4}$$

where α_m is the same as α_n. The total harvested power (HP) for user m is $P_{k,m}(T_k, s_k)$ summed $\forall \ k$. For the allocation over the entire OFDM symbol, the total transmit power constraint must also be considered.

3. OPTIMUM RESOURCE ALLOCATION

3.1. Primal Maximization

The resource allocation problem is formulated as the maximization of a weighted sum of DRs over all users and sub-carriers, subject to the total transmit power constraint P_{Total} and the minimum per-user harvested power C_m, and is given as

$$\begin{aligned} \underset{\{T_k, s_k\} \forall k}{\text{maximize}} & \sum_{k=1}^{K} \sum_{n=1}^{N} \omega_n \log_2 \left(1 + \gamma_{k,n}^{\mathrm{DS}}(T_k, s_k)\right) \\ \text{Subject to} & \sum_{k=1}^{K} P_{k,m}(T_k, s_k) \geq C_m \ \forall \ m \in [1, ..., N] \\ & \sum_{k=1}^{K} \sum_{n=1}^{N} s_{k,n} ||t_{k,n}||_2^2 \leq P_{\mathrm{Total}}. \end{aligned} \tag{5}$$

The optimal point is chosen by selecting a precoder matrix ($T_k \ \forall \ k$) and symbol power vector ($s_k \ \forall \ k$) which maximizes the weighted sum. The weights ω_n are used to weight the importance of individual user DRs as determined by the use-case.

3.2. Lagrange Dual

Dual decomposition is used to split the primal problem in (5) into K smaller problems to be solved in parallel, and enables the use of MAC-BC duality theory. The dual problem is formulated by dualizing the constraints and combining them with the objective function.

The Lagrange dual function is defined as

$$q(\lambda) \triangleq \underset{T,s}{\text{maximize}} \, \mathcal{L}(s, T, \lambda) \tag{6}$$

where the Lagrangian, $\mathcal{L}(\mathbf{s}, \mathbf{T}, \boldsymbol{\lambda})$, is

$$\begin{aligned} \mathcal{L}(s, T, \lambda) = \lambda_0 P_{\mathrm{Total}} - \sum_{m=1}^{N} \lambda_m C_m + \\ \sum_{k=1}^{K} \sum_{n=1}^{N} \omega_n \log_2(1 + \gamma_{k,n}^{\mathrm{DS}}(T_k, s_k)) - \\ \sum_{k=1}^{K} \sum_{n=1}^{N} t_{k,n}^{\mathcal{H}} (\lambda_0 I - \sum_{m=1}^{N} \lambda_m (h_{k,m} h_{k,m}^{\mathcal{H}})) t_{k,n} s_{k,n}, \end{aligned} \tag{7}$$

and $\boldsymbol{\lambda} = [\lambda_0, ..., \lambda_N]^T$. Additionally we will define $\Upsilon_k(\boldsymbol{\lambda})$ as:

$$\Upsilon_k(\lambda) \triangleq \left(\lambda_0 I - \sum_{m=1}^{N} \lambda_m h_{k,m} h_{k,m}^{\mathcal{H}}\right). \tag{8}$$

If $\Upsilon_k(\boldsymbol{\lambda})$ is not positive definite for all k then (6) will become unbounded and $q(\boldsymbol{\lambda})$ will be $+\infty$, in which case the corresponding $\boldsymbol{\lambda}$ cannot be dual optimal. The Lagrange dual problem is then given by

$$\begin{aligned} \underset{\lambda}{\text{minimize}} \quad & q(\lambda) \\ \text{Subject to} \quad & \lambda \geq 0 \\ & \Upsilon_k(\lambda) \succ 0 \ \forall \ k. \end{aligned} \tag{9}$$

Note that the primal problem in (5) is not convex and so the duality gap may be non-zero. A non-zero duality gap would mean that a solution to the dual problem is not guaranteed to lead to an optimal solution for the primal problem. However, [7] indicates that the time-sharing property of a practical multi-carrier system provides for zero duality gap.

3.3. Dual Function Evaluation

MAC-BC duality allows the construction of a multiple access channel (MAC) problem that has a known solution [8] linked to the solution of the BC maximization problem ($\forall \ k$) in (6). The duality asserts that provided $\Upsilon_k(\boldsymbol{\lambda}) \succ 0$, then for any positive $\boldsymbol{s_k}$ and $\mathbf{T_k}$ there exists a dual SP vector ($\boldsymbol{\delta_k}$) that achieves the same SINR in the MAC (upstream channel $\mathbf{H_k}$ with encoder $\mathbf{T}_\mathbf{k}^{\mathcal{H}}$) as in the BC (downstream channel $\mathbf{H}_\mathbf{k}^{\mathcal{H}}$ with precoder $\mathbf{T_k}$). In our case, we will convert our BC problem to a MAC problem by equating the SINRs, optimize over the dual SPs, solve for the optimal equalizer, and then convert back to attain the optimal precoder. Equating the SINRS results in

$$\gamma_{k,n}^{\mathrm{DS}}(T_k, s_k) = \gamma_{k,n}^{\mathrm{US}}(T_k, \delta_k), \ \forall \ k \text{ and } n, \tag{10}$$

where $\gamma_{k,n}^{\mathrm{DS}}(\mathbf{T_k}, \boldsymbol{s_k})$ is defined in (3) and the dual upstream (US) SINR is given by:

$$\gamma_{k,n}^{\mathrm{US}}(T_k, \delta_k) = \frac{|t_{k,n}^{\mathcal{H}} h_{k,n}|^2 \delta_{k,n}}{\sum_{\substack{m=1 \\ m \neq n}}^{N} |t_{k,n}^{\mathcal{H}} h_{k,m}|^2 \delta_{k,m} + t_{k,n}^{\mathcal{H}} \Upsilon_k(\lambda) t_{k,n}}. \tag{11}$$

In (11), $\boldsymbol{\delta_k}$ is the SP vector in the US system and $\Upsilon_k(\boldsymbol{\lambda})$ is seen to act as a noise covariance matrix. Since $\Upsilon_k(\lambda) \succ 0$, (10) may be expressed as:

$$Z_k s_k = \sigma_k \circ \delta_k, \tag{12}$$

where $\circ$ is the Hadamard product and $\mathbf{Z_k}$ is given by:

$$\begin{aligned} [Z_k]_{ij} &= \sum_{\substack{n=1 \\ n \neq j}}^{N} |t_{k,j}^{\mathcal{H}} h_{k,n}|^2 \delta_{k,n} + t_{k,j}^{\mathcal{H}} \Upsilon_k(\lambda) t_{k,j}, \text{ for } i = j \\ [Z_k]_{ij} &= -\delta_{k,i} |t_{k,j}^{\mathcal{H}} h_{k,i}|^2, \text{ for } i \neq j. \end{aligned} \tag{13}$$

$\mathbf{Z_k}$ is an M-matrix [9]. Therefore, it is guaranteed that for any $\boldsymbol{\delta_k} \geq 0$, solving (12) yields a $\boldsymbol{s_k} \geq 0$. Summing the rows of (12) yields:

$$\sum_{n=1}^{N} t_{k,n}^{\mathcal{H}} \Upsilon_k(\lambda) t_{k,n} s_{k,n} = \sigma_k^{\mathcal{H}} \delta_k. \tag{14}$$

The maximization problem ($\forall \ k$) in (6) may then be simplified further by redefining the problem in terms of the dual upstream DR and using (14) to arrive at:

$$\underset{T_k, \delta_k}{\text{maximize}} \quad \sum_{n=1}^{N} \omega_n \log_2(1 + \gamma_{k,n}^{\mathrm{US}}(T_k, \delta_k)) - \sigma_k^{\mathcal{H}} \delta_k. \tag{15}$$

3.4. Equalizer Optimization

Equation (15) is separable when maximizing over $\mathbf{T_k}$ (given $\boldsymbol{\delta_k}$) since the SINR of user n (given by $\gamma_{k,n}^{\mathrm{US}}$) only depends on the receive filter ($\boldsymbol{t_{k,n}}$) of user n and $\boldsymbol{\sigma_k^{\mathcal{H}}\delta_k}$ does not. This, along with the monotonicity of $log(1+\cdot)$, allows us to only consider $\gamma_{k,n}^{\mathrm{US}}(\mathbf{T_k}, \boldsymbol{\delta_k})$ in the maximization:

$$\underset{T_k}{\text{maximize}} \quad \gamma_{k,n}^{\mathrm{US}}(T_k, \delta_k). \tag{16}$$

The optimal linear equalizer for a MAC is the linear MMSE equalizer and, given the US SINR in (11), is readily shown to be:

$$t_{k,n}^{*} = (\sum_{\substack{m=1 \\ m\neq n}}^{N} \delta_{k,m} h_{k,m} h_{k,m}^{\mathcal{H}} + \Upsilon_k(\lambda))^{-1} h_{k,n}. \tag{17}$$

The expression in (17) enables the dual upstream SINR to be expressed as only a function of $\boldsymbol{\delta_k}$, i.e.

$$\gamma_{k,n}^{\mathrm{US}}(\delta_k) = \delta_{k,n} h_{k,n}^{\mathcal{H}} \left[\sum_{\substack{m=1 \\ m\neq n}}^{N} \delta_{k,m} h_{k,m} h_{k,m}^{\mathcal{H}} + \Upsilon_k(\lambda) \right]^{-1} h_{k,n}. \tag{18}$$

3.5. Dual Symbol Power Optimization

Successive convex approximation [10] is employed to optimize the dual SP vector ($\boldsymbol{\delta_k}$). Successive approximations of (15) are made by fixing constant the dual upstream SP values $\delta_{k,m}$ of all users $m \neq n$ and by approximating the DRs with their first order Taylor expansion for all users $m \neq n$. This leads to the maximization being approximated with:

$$\begin{aligned} \underset{\delta_{k,n}}{\text{maximize}} \quad & \omega_n \log_2(1 + \delta_{k,n}\bar{q}_{k,n}) - (\bar{\phi}_{k,n} + \sigma_{k,n})\delta_{k,n} \\ \text{Subject to} \quad & \delta_{k,n} \geq 0, \end{aligned} \tag{19}$$

where $\bar{q}_{k,n}$ is the interference-plus-noise covariance,

$$\bar{q}_{k,n} = h_{k,n}^{\mathcal{H}} \left[\sum_{\substack{m=1 \\ m\neq n}}^{N} \bar{\delta}_{k,m} h_{k,m} h_{k,m}^{\mathcal{H}} + \Upsilon_k(\lambda) \right]^{-1} h_{k,n}, \tag{20}$$

$\bar{\phi}_{k,n}$ is from the first order Taylor series expansion,

$$-\bar{\phi}_{k,n} = \frac{\partial}{\partial \delta_k} [\sum_{\substack{m=1 \\ m\neq n}}^{N} \omega_m log_2(1 + \gamma_{k,m}^{\mathrm{US}}(\delta_k))] \Big|_{\delta_k = \bar{\delta}_k}, \tag{21}$$

and $\sigma_{k,n}$ is the noise. Terms that are constant over the maximization were removed from the approximation. KKT conditions enable calculating the optimal value for $\delta_{k,n}$ via the following equation:

$$\delta_{k,n}^{*} = \left[0, \frac{\frac{\omega_n}{log(2)}}{\bar{\phi}_{k,n} + \sigma_n} - \frac{1}{\bar{q}_{k,n}} \right]^{+}, \tag{22}$$

where $[x, y]^{+} = \max\{x, y\}$.

3.6. Solving the Dual Problem

Since (9) is convex, the deep-cut ellipsoid algorithm can be used to find values for $\boldsymbol{\lambda}$ as described in [11]. Once $\boldsymbol{\lambda}$ is selected, the resource allocation solves for the optimal dual SP, which is then used to calculate the optimal precoder and SP for the BC. This is done iteratively until convergence.

3.6.1. Ellipsoid Initialization

An ellipsoid $\mathcal{E}$ can be described as $\mathcal{E} = \{\boldsymbol{z} \mid (\boldsymbol{z}-\boldsymbol{\lambda})^T \mathbf{P}^{-1} (\boldsymbol{z}-\boldsymbol{\lambda}) \leq 1\}$, where $\boldsymbol{\lambda}$ is the center of the ellipsoid and $\mathbf{P}$ gives the size and shape of $\mathcal{E}$. The initial ellipsoid may be defined with $\mathbf{P} = \boldsymbol{\lambda_{UB}^2}\mathbf{I}$, where $\boldsymbol{\lambda_{UB}}$ is an $N+1\times 1$ vector of upper-bounds for the optimal $\boldsymbol{\lambda}$. The center for each successive ellipsoid defines $\boldsymbol{\lambda}$ for each iteration.

3.6.2. Upper-bound for Lagrange Multipliers

Since $q(\boldsymbol{\lambda})$ is minimized when $\boldsymbol{\lambda} = \boldsymbol{\lambda^*}$, any other $\boldsymbol{\lambda}$ would result in a larger value for $q(\boldsymbol{\lambda})$, yielding

$$q(\lambda) \geq q(\lambda^*). \tag{23}$$

Similarly, if $s = s^*$ and $T = T^*$ maximizes $\mathcal{L}(s, T, \lambda)$ then any other s and T (provided that $s \geq 0$) will yield a smaller $\mathcal{L}$, giving

$$\mathcal{L}(s, T, \lambda) \leq \mathcal{L}(s^*, T^*, \lambda). \tag{24}$$

Using an approach detailed in [12] (p. 43), (23) and (24) are reformulated to solve for the $\boldsymbol{\lambda^*}$ upper-bound. The equation is further modified by plugging in values for a feasible $\mathbf{s} = \mathbf{s}^{'}$ and $\mathbf{T} = \mathbf{T}^{'}$ as well as the solution for $q(\lambda)$ when $\boldsymbol{\lambda} = [1, ..., 1]^T$. This yields an expression for the λ_m^* upper-bound:

$$\lambda_m^* \leq \frac{q(1) - \sum_{k=1}^{K} \sum_{n=1}^{N} \omega_n \log_2(1 + \gamma_{k,n}^{\mathrm{DS}}(T_k^{'}, s_k^{'}))}{P_m(s^{'}, T^{'}) - C_m}, \tag{25}$$

as well as one for the λ_0^* upper-bound:

$$\lambda_0^* \leq \frac{q(1) - \sum_{k=1}^{K} \sum_{n=1}^{N} \omega_n \log_2(1 + \gamma_{k,n}^{\mathrm{DS}}(T_k^{'}, s_k^{'}))}{P_{Total} - \sum_{k=1}^{K} \sum_{n=1}^{N} s_{k,n}^{'} ||t_{k,n}^{'}||_2^2}. \tag{26}$$

Feasible $\mathbf{s}^{'}$ and $\mathbf{T}^{'}$ are found by minimizing the transmit power subject to meeting the constraints to the primal problem (5), which can be posed as a semidefinite program:

$$\begin{aligned} \underset{\{Q_k^{\mathcal{H}}\}_{\forall k}}{\text{minimize}} \quad & \sum_{k}^{K} < Q_k^{\mathcal{H}}, I > \\ \text{Subject to} \quad & \sum_{k=1}^{K} < Q_k^{\mathcal{H}}, (h_{k,m} h_{k,m}^{\mathcal{H}}) > \geq \ C_m \ \forall \ m \\ & Q_k \succcurlyeq 0 \ \forall \ k, \end{aligned} \tag{27}$$

where $\mathbf{Q_k} \triangleq \sum_n^N \boldsymbol{t_{k,n}} s_{k,n} \boldsymbol{t_{k,n}^{\mathcal{H}}} = \mathbf{T_k} \boldsymbol{s_k} \mathbf{I_{NxN}} \mathbf{T_k^{\mathcal{H}}}$ and $< \mathbf{A}, \mathbf{B} > \triangleq trace(\mathbf{A}^{\mathcal{H}}\mathbf{B})$ is the Frobenius inner product. By setting $\boldsymbol{s_k^{'}} = 1 \ \forall \ k$, $\mathbf{T_k^{'}}$ may be found by factoring $\mathbf{Q_k}$. The upper-bound for $\boldsymbol{\lambda}$ can then be calculated and used to initialize the ellipsoid algorithm.

3.6.3. Ellipsoid Cuts

The deep-cut ellipsoid method iteratively reshapes the ellipsoid using either a feasibility cut or an objective cut. A feasibility cut is made when a dual constraint (specified in (9)) is violated and is based on the normalized subgradient of the violated constraint. Entries associated with the non-violated constraints are set to zero. The Lagrange multiplier constraint function is of the form:

$$m_n(\lambda) = -\left[0, ..., \lambda_n, ..., 0\right]^T. \tag{28}$$

The subgradient of the Lagrange multiplier constraint function is of the form:

$$\nabla m_n(\lambda) = \left[0, ..., -1, ..., 0\right]^T. \tag{29}$$

The constraint associated with $\Upsilon_k(\boldsymbol{\lambda})$ is equivalent to

$$f_k(\lambda) = \lambda_0 - \max\{\text{ eigenvalues } \{\sum_m^N \lambda_m h_{k,m} h_{k,m}^{\mathcal{H}}\}\} \geq 0 \; \forall \; k. \tag{30}$$

If $\boldsymbol{\upsilon_\sigma}$ is the normalized eigenvector related to the maximum eigenvalue of $\sum_m^N \lambda_m \boldsymbol{h_{k,m}} \boldsymbol{h_{k,m}^{\mathcal{H}}}$, then the subgradient [13] of $f_k(\lambda)$ is:

$$\nabla f_k(\lambda) = \begin{bmatrix} \frac{\partial f(\lambda)}{\partial \lambda_0} \\ \frac{\partial f(\lambda)}{\partial \lambda_1} \\ \vdots \\ \frac{\partial f(\lambda)}{\partial \lambda_N} \end{bmatrix} = \begin{bmatrix} 1 \\ -||h_{k,1}^{\mathcal{H}} \upsilon_\sigma||_2^2 \\ \vdots \\ -||h_{k,N}^{\mathcal{H}} \upsilon_\sigma||_2^2 \end{bmatrix}. \tag{31}$$

An objective cut is made when the dual constraints are met but the primal constraints are not. The objective cut is based on the subgradient of the objective function (6) and is:

$$\nabla \mathcal{L}(s, T, \lambda) = \begin{bmatrix} P_{\text{tot}} - \sum_{k=1}^K \sum_{n=1}^N t_{k,n}^{\mathcal{H}} t_{k,n} s_{k,n} \\ -C_1 + \sum_{k=1}^K \sum_{n=1}^N t_{k,n}^{\mathcal{H}} (h_{k,1} h_{k,1}^{\mathcal{H}}) t_{k,n} s_{k,n} \\ \vdots \\ -C_N + \sum_{k=1}^K \sum_{n=1}^N t_{k,n}^{\mathcal{H}} (h_{k,N} h_{k,N}^{\mathcal{H}}) t_{k,n} s_{k,n} \end{bmatrix}. \tag{32}$$

The optimal $\mathbf{s}$ and $\mathbf{T}$ are obtained via a method outlined in (3.3).

4. SIMULATIONS

A network of remote devices receiving data and power from one access point is modeled to show the resource allocation algorithm meeting its data rate and energy consumption needs. A simple method from queue stability theory is used to determine the DR weights, ω_n, and the HP constraints, C_n. In particular, instead of predetermining a constant C_n for each device, the perturbed queue size is used to dynamically choose these values.

4.1. Network Model

The network operates in slotted time and each device has a data queue and energy queue. The data queues are located at the access point and store data before transmitting to a specific device. The size of the data queue at slot $t+1$ for device n may be modeled with

$$Q_n(t+1) = [0, Q_n(t) - R_n(t)]^+ + A_n(t), \tag{33}$$

where $Q_n(t)$ is the value of the queue in bits, $R_n(t)$ is the amount of data transmitted to the device, and $A_n(t)$ is the amount of data added to the queue. An energy queue is located at each remote device n for energy storage, the size of which at slot $t+1$ may be modeled as

$$B_n(t+1) = [0, B_n(t) - D_n(t)]^+ + E_n(t), \tag{34}$$

where $B_n(t)$ is the value of the queue in joules, $D_n(t)$ is the amount of energy consumed by the device, and $E_n(t)$, given by

$$E_n(t) = \tau \sum_{k=1}^K P_{k,n}(T_k(t), s_k(t)), \tag{35}$$

is the amount of energy added to the queue. τ is the slot duration in seconds. $T_k(t)$ and $s_k(t)$ are determined at the beginning of slot t. Neither queue type is allowed to be negative. The data arrival rates, $A_n(t)$, follow a Poisson distribution with a mean value that is within the rate region. The energy consumption rates, $D_n(t)$, are kept constant.

4.2. Setting Resource Allocation Parameters

Max-Weight scheduling has been shown to stabilize network queues for systems using a linear sum of weighted attributes for resource allocation [14], which is the type of formulation this paper uses. Based on Max-Weight scheduling, the DR weights are assigned the queue size, i.e.

$$\omega_n(t+1) = [1, Q_n(t+1)]^+ \; \forall \; n, \tag{36}$$

and the minimum HP is assigned the perturbed queue size, i.e.

$$C_n(t+1) = \theta_n - B_n(t+1) \; \forall \; n, \tag{37}$$

where θ_n is a target value [15]. Other parameters are in the footnote[1].

4.3. Results

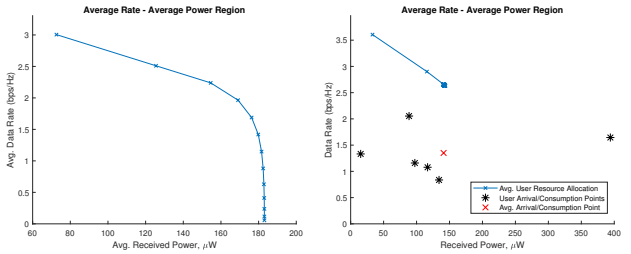

(a) Projected Paretto Edge (b) Simulation Operating Points

Fig. 1. Projected Rate-Power Region

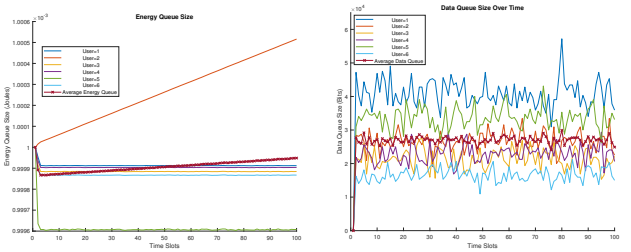

(a) Energy Queue (b) Data Queue

Fig. 2. Queue Dynamics

Fig.1(a) shows the edge of the projected rate-power region. Fig.1(b) illustrates the network operating points for the simulation, which shows that the amount of power allocated (x-axis, blue markers) to the network quickly becomes tight to the average network power consumption (x-axis, red x), but provides a higher DR than is required (y-axis). This is due to the allocation maximizing the network DR once the HP constraints are met. That is, once the resource allocation stabilizes the energy queues (depicted in Fig.2(a)) the operating points adjust to meet the changing data arrival rates and stabilizes the data queues such that they don't grow indefinitely as depicted in Fig. 2(b).

[1]Simulation parameters: $K = 64$, $N_T = N = 6$, sub-carrier bandwidth of 312.5 kHz, OFDM bandwidth of 20 MHz, $P_{Total} = 50$ dBm, large scale pathloss is 30 dB, $\sigma_n = -112$ dBm, $\tau = 0.001$ seconds, and the network experiences a Rayleigh fading environment [16]. At $t = 0$, the data queue $Q_n(t) = 0$ bits, the energy queue $B_n(t) = 1$ mJ, and $\theta_n = 1.000001$ mJ $\forall \; n$.

5. REFERENCES

[1] Weidang Lu, Yi Gong, Jiaying Wu, Hong Peng, and Jingyu Hua, "Simultaneous Wireless Information and Power Transfer Based on Joint Subcarrier and Power Allocation in OFDM Systems," vol. 5, pp. 2763–2770, 2017.

[2] K. Huang and E. Larsson, "Simultaneous Information and Power Transfer for Broadband Wireless Systems," vol. 61, no. 23, pp. 5972–5986, Dec. 2013.

[3] Z. B. Zawawi, J. Park, and B. Clerckx, "Simultaneous Wireless Information and Power Transfer in a two-user OFDM Interference Channel," in *2015 International Symposium on Wireless Communication Systems (ISWCS)*, Aug. 2015, pp. 266–270.

[4] Jie Xu, Liang Liu, and Rui Zhang, "Multiuser MISO Beamforming for Simultaneous Wireless Information and Power Transfer," vol. 62, no. 18, pp. 4798–4810, Sept. 2014.

[5] Q. Shi, L. Liu, W. Xu, and R. Zhang, "Joint Transmit Beamforming and Receive Power Splitting for MISO SWIPT Systems," vol. 13, no. 6, pp. 3269–3280, June 2014.

[6] Zhengyu Zhu, Zhongyong Wang, Xin Gui, and Xiangchuan Gao, "Robust downlink beamforming and power splitting design in multiuser MISO SWIPT system," in *2014 IEEE/CIC International Conference on Communications in China (ICCC)*, Shanghai, China, Oct. 2014, pp. 271–275.

[7] Wei Yu and R. Lui, "Dual methods for nonconvex spectrum optimization of multicarrier systems," vol. 54, no. 7, pp. 1310–1322, July 2006.

[8] R. Hunger, M. Joham, and W. Utschick, "On the MSE-Duality of the Broadcast Channel and the Multiple Access Channel," vol. 57, no. 2, pp. 698–713, Feb. 2009.

[9] David Tse and Pramod Viswanath, *Fundamentals of Wireless Communication*, Cambridge University Press, 2005.

[10] Gesualdo Scutari, Francisco Facchinei, Peiran Song, Daniel P. Palomar, and Jong-Shi Pang, "Decomposition by Partial Linearization: Parallel Optimization of Multi-Agent Systems," vol. 62, no. 3, pp. 641–656, Feb. 2014.

[11] Martin Grötschel, László Lovász, and Alexander Schrijver, *Geometric Algorithms and Combinatorial Optimization*, Number 2 in Algorithms and Combinatorics. Springer, Berlin, 1988, OCLC: 17299859.

[12] Johannes Brehmer, *Utility Maximization in Nonconvex Wireless Systems*, Number 5 in Foundations in Signal Processing, Communications and Networking. Springer, Berlin, 2012, OCLC: 801307163.

[13] Karim T. Abou–Moustafa, "On Derivatives of Eigenvalues and Eigenvectors of the Generalized Eigenvalue Problem," Tech. Rep. TR–CIM–10–10, Centre of Intelligent Machines, McGill University, Montréal, Canada, 2010.

[14] Michael Neely, *Stochastic Network Optimization with Application to Communication and Queueing Systems*, Morgan & Claypool, 2010.

[15] L. Huang and M. J. Neely, "Utility Optimal Scheduling in Energy-Harvesting Networks," vol. 21, no. 4, pp. 1117–1130, Aug. 2013.

[16] J. Medbo and P. Schramm, "Channel models for HIPERLAN/2 in different indoor scenarios," vol. 3ERI085B, Mar. 1998.